IEICE TRANS. COMMUN., VOL.E106–B, NO.9 SEPTEMBER 2023

PAPER Special Section on Technologies and Proof-of-Concept Activities for 5G Advanced and 6G

Proof of Concept of Optimum Radio Access Technology Selection Scheme with Radars for Millimeter-Wave Networks

Mitsuru UESUGI[†a)], **Yoshiaki SHINAGAWA**[†], ***Members***, **Kazuhiro KOSAKA**[†], **Toru OKADA**[†], **Takeo UETA**[†], ***and*** **Kosuke ONO**[†], ***Nonmembers***

SUMMARY With the rapid increase in the amount of data communication in 5G networks, there is a strong demand to reduce the power of the entire network, so the use of highly power-efficient millimeter-wave (mm-wave) networks is being considered. However, while mm-wave communication has high power efficiency, it has strong straightness, so it is difficult to secure stable communication in an environment with blocking. Especially when considering use cases such as autonomous driving, continuous communication is required when transmitting streaming data such as moving images taken by vehicles, it is necessary to compensate the blocking problem. For this reason, the authors examined an optimum radio access technology (RAT) selection scheme which selects mm-wave communication when mm-wave can be used and select wide-area macro-communication when mm-wave may be blocked. In addition, the authors implemented the scheme on a prototype device and conducted field tests and confirmed that mm-wave communication and macro communication were switched at an appropriate timing.

key words: *millimeter-wave, power efficiency, radar, communication quality prediction, radio access technology (RAT)*

1. Introduction

As the 5G system became widespread, it has become possible to realize services that require high-speed, low-latency communication. However, as the number of use cases that require such a large amount of data increases, the power consumption of 5G networks become enormous, and it is essential to improve power efficiency. For this reason, we are trying to add "non-3GPP access" over 5G system for the purpose of the improvement capacity and power consumption of the system. We use millimeter wave (hereafter abbreviated as "mm-wave") Wireless Local Area Network (WLAN) using 60 GHz band, which standardized in IEEE802.11ad [1] and can achieve multi-gigabit data rates and is expected to ensure interoperability, as the non-3GPP access [2]. The target use cases which aim to use for next-generation Intelligent Transport Systems (ITS) are following [3], and this report is regarding mainly about (1) as shown in Fig. 1:

(1) Real time and continuous video streaming which used for remote monitoring

(2) Download huge size data, such as 3D map and so on.

Since mm-wave communication (hereafter abbreviated as "mm-com") is highly power-efficient and consumes less power per bit, it may improve the power efficiency of the 5G system if install mm-wave spots in areas with high traffic and use mm-com as much as possible. However, mm-wave has a strong straightness, and if there is blocked line of sight between transmission and reception, there is a problem that communication may be cut off because it cannot go around the blocking objects. Therefore, there are many studies are underway to improve power efficiency by applying mm-wave to 5G networks [4]–[7] and have been tried to compensate the issue.

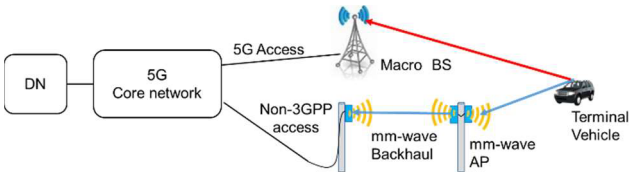

Fig. 1 The use case (1): Real time and continuous video streaming which used for remote monitoring.

The authors added an original estimating scheme when to enter the blocked area by detecting the position of the terminal using a mm-wave radar and estimating the future position of the terminal based on the detection result for the previous scheme shown in [8]. Using this scheme, it is possible to switch Radio Access Technology (RAT) from mm-com to macro communication (hereafter abbreviated as "macro-com") just before the terminal enters the blocked area and return to mm-com immediately after the terminal leaves the blocked area. Therefore mm-com can be used to the maximum without interruption making it possible.

To realize this scheme, it is required being able to accurately realize object detection and route prediction using mm-wave radar, and necessary to have the accuracy of determining the optimum RAT switching timing using the route prediction results. The former has realized wide-area and highly accurate route prediction by using multiple mm-wave radars and combining their detection results with a Kalman filter [9]. In addition, the latter has realized RAT selection without interruption even in an environment where a blocking area is existed by using a quality map that reflects road conditions.

The authors also implemented the scheme on experimental equipment and verified the effectiveness of the scheme in real field. The result of that show when the pro-

Manuscript received September 30, 2022.
Manuscript revised January 16, 2023.
Manuscript publicized May 23, 2023.

[†]The authors are with Panasonic Connect Co., Ltd., Yokohama-shi, 224-8539 Japan.
a) E-mail: uesugi.mitsuru@jp.panasonic.com

DOI: 10.1587/transcom.2022FGP0001

posed RAT selection scheme is used, no interruption RAT selection can be done in not only in wide area field but also in many multi path environment as in urban model.

2. Optimum RAT Selection Scheme

2.1 Issues and Solutions of the Mm-Wave Network

A network composed of mm-waves, communication is interrupted when the mm-wave access line is blocked by blocking objects such as parked vehicle or the like. For this reason, in use cases where continuous communication is required, such as uploading (UL) moving images, as shown in Fig. 2, the macro-com covering a wide area is configured to overlap the mm-wave network. The proposed scheme can select mm-com which is highly power efficient when the terminal is in an area where mm-com is possible, and macro-com when it is in an area where mm-waves are blocked, then high power efficiency is satisfied. At that time, in use cases where continuous communication is required, it is also required that momentary interruptions and data loss do not occur when switching between mm-com and macro-com.

2.2 RAT Selection of Terminal-Driven

The simplest scheme for selecting RAT described in the previous section is that RAT selection at a terminal itself. In the terminal, the mm-com is preferentially selected in the area where the mm-com can be used. Therefore, the terminal constantly monitors the communication quality of mm-com, and switch from mm-com to macro-com when the quality drops below a target threshold, and conversely from macro-com to mm-com when it recovers above the threshold. Hereinafter, this scheme is referred to as "terminal-driven". However, in this scheme, since switching is performed after the mm-com is cut off, there is a possibility that a momentary interruption may occur when switching from mm-com to macro-com. Therefore, in the next section, we examined a scheme that does not cause a momentary interruption.

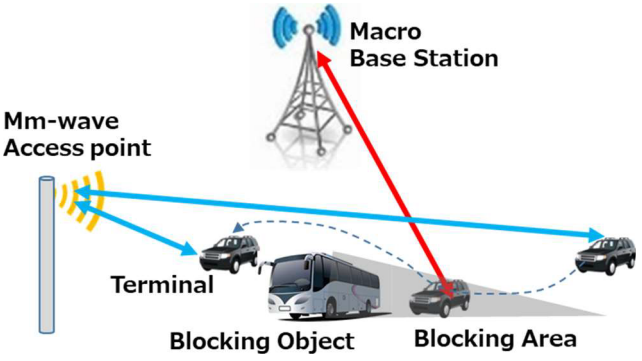

Fig. 2 Overlap configuration of mm-wave network and macro-com.

2.3 RAT Selection of GW-Driven

There has been a lot of literature on blocking, which is the biggest issue of mm-waves, for a long time, and analysis of dynamic channel models of blocking has also been performed [10]. In addition, schemes of predicting blocking and consequent received signals by incorporating machine learning [11] and schemes of performing handover between multiple base stations by machine learning [12] are being studied. However, because they are not to cope with temporary blocking by parked vehicles, etc., the authors devised a new scheme that uses prediction of switching time based on terminal detection by mm-wave radar using 79 GHz band and dynamic quality map. In this scheme, it is possible to predict when the terminal will go to the place where mm-com will be cut off, so it can switch to macro-com in advance. Since in the scheme, 5G Gate Way (5G-GW) performs terminal position detection and communication quality prediction, and it notifies to the terminal of the switching timing to switch, this scheme is referred to as "GW-driven" below.

3. Implementation of GW-Driven Scheme

3.1 Detection and Route Prediction for a Terminal

To realize the GW-driven, it is necessary to detect the position of the terminal sequentially, so we decided to use mm-wave radar. Since mm-com is possible to connect to a distance about 150 m, the detection of the terminal should also cover the area from 5G-GW to around 150 m. However, since the detection range of a radar device assuming to use was about 60 m, three radars were arranged in a row at 50 m intervals as shown in Fig. 3 to enable detection up to around 150 m [9].

3.2 Optimum RAT Selection Using Quality Map

If the position of the terminal can be detected sequentially by the mm-wave radar, the route of the future terminal is predicted using the result, and the communication quality in that route can be obtained. To predict the communication quality, 5G-GW has a dynamic quality map, that is made not only the calculation by the simple two paths model of mm-com but also considered the influence from parked vehicles

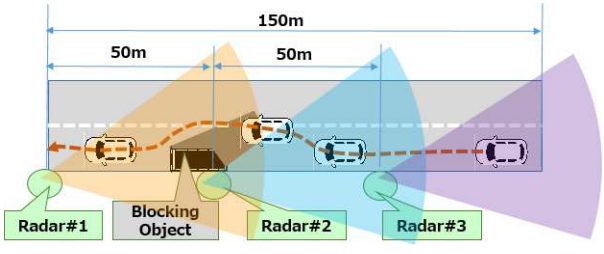

Fig. 3 Terminal detection using three radars.

and so on. This makes it possible to predict in consideration of changes in the dynamic environment when the terminal will reach the area where mm-com is blocked. Therefore, by notifying the terminal of that time, it can switch to macro-com before down the mm-com. Note that we have confirmed the time to switch of RAT by GW-driven is about 35 ms both from mm-com to macro-com and from macro-com to mm-com.

4. Verification with a Prototype Equipment

4.1 Outline of the Prototype Equipment

To verify the RAT selection schemes examined in the previous section, both terminal-driven and GW-driven scheme were mounted on the prototype device, and field tests were conducted for comparison. Fig. 4 shows the block diagram of the prototype equipment.

At the terminal vehicle, there are PC to control the terminal, two cameras to capture the streaming images of the front and back of the terminal, mm-wave terminal, and macro terminal. PC switches to use one of the mm-wave terminal or macro terminal by the control signal from 5G-GW.

5G-GW has LSS (Local Service Server) to hold the huge size data for the download, mm-wave AP (Access Point), and three radars as written in Sect. 3.1.

SS (Service server) receives streaming data both from macro-BS (Base Station) and mm-wave AP through 5G-GW. It combines the data from them to one streaming image.

4.2 Condition of the Field Test of the First Trial

To confirm basic performance, field tests were conducted in a fully insight environment with no reflectors at first. Figure 5, Fig. 6, Fig. 7, and Fig. 8 show the position of each device on the field, the experimental scene, the terminal vehicle, and the items at 5G-GW, respectively. The rear edge of the blocking object (large and parked vehicle which has aluminum container at the rear part with about 3 m high) was set to the point of 50 m from 5G-GW as shown in Fig. 5, where just the same position as the second radar (radar #2). The terminal took a moving image and uploaded it continuously as streaming data of FHD 60 fps M-JPEG with about

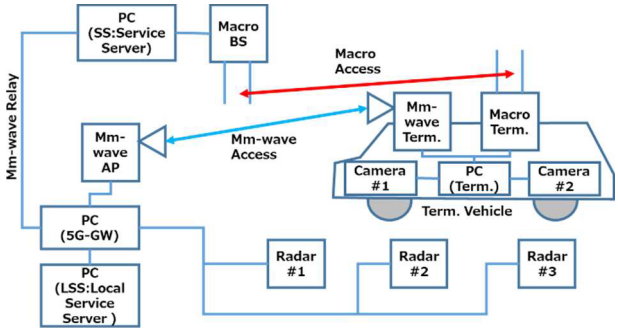

Fig. 4 Block diagram of the prototype equipment.

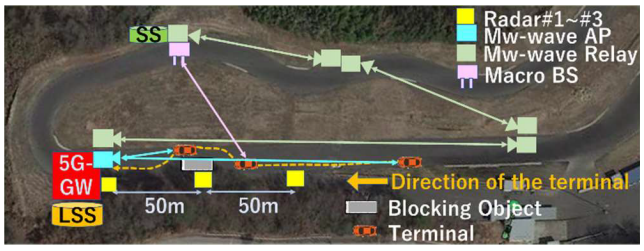

Fig. 5 Position of each device on the field.

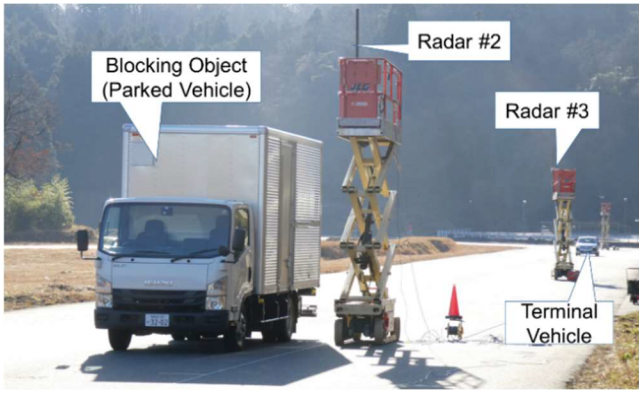

Fig. 6 The experimental scene.

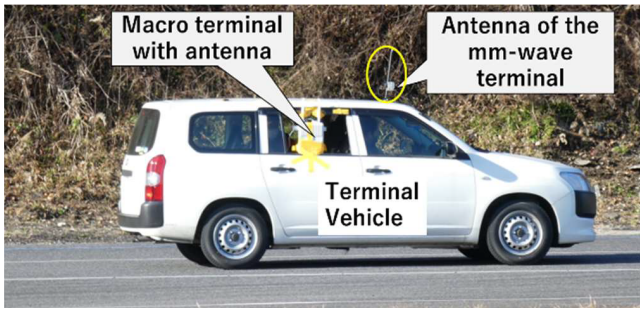

Fig. 7 The terminal vehicle (terminal 1).

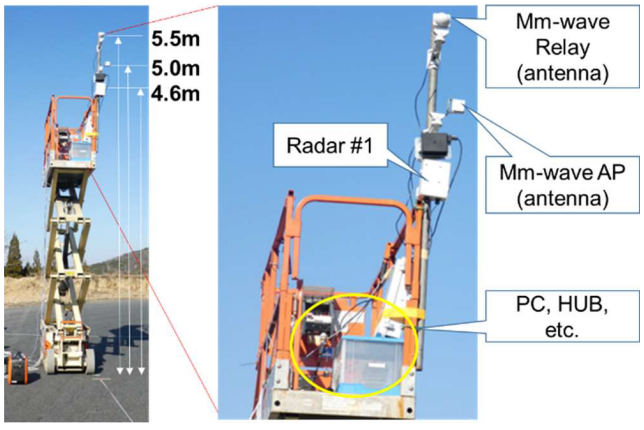

Fig. 8 The items at 5G-GW.

120 Mbps during mm-com and VGA 30 fps M-JPEG with about 6.5 Mbps during macro-com. The data was sent to the mm-wave AP at the 5G-GW when using mm-com, and then sent to SS through mm-wave relays, and the data sent to SS through macro-BS when using macro-com. On the other hand, when downloading the stored data all at once, the large amount of data, such as 3D map information etc., stored in the LSS (Local Service Server) of 5G-GW was transmitted from the mm-wave AP and received by the terminal.

In addition, since the mm-wave blocked area by the blocking object exists from 5G-GW to the vicinity up to 81 m, the overtaking points are set to 3 points of 60 m, 74 m, 83 m from 5G-GW as shown in Fig. 9. In this experiment, the load on the 5G-GW CPU was heavy due to set many points where logs were acquired in to analyze the phenomenon, and the size of the experiment field was not so wide. Therefore, the terminal vehicle shown in Fig. 7 was limited to the speed about 10 km/h. In this experiment, Wi-Fi (2.4 GHz/5 GHz) was used as a substitute for macro-com.

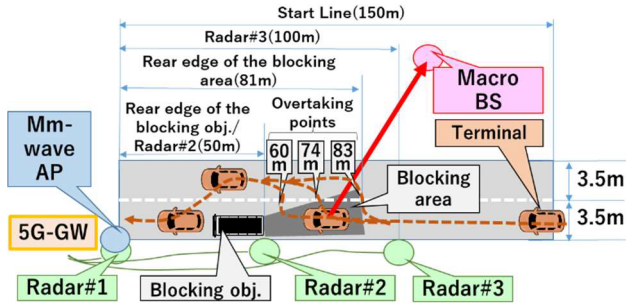

Fig. 9 Three routes of the terminal vehicle.

4.3 Comparison of the Performance of Selection Schemes

Figure 10 and Fig. 11 are results of terminal-driven and GW-driven experimental results at overtaking points 60 m, 74 m, and 83 m, respectively. Because overtaking point of (a), (b), and (c) is different, position of the terminal is different even if the same horizontal distance from 5G-GW in Fig. 10. Therefore, the effect of blocking is the smallest for (c), the momentary interruption, which is defined as the case where the throughput of 0 continues twice (200 ms) or more, near 80 m seen in (a) and (b) could not be confirmed in (c). Another point worth noting is that throughput may appear to drop to 0 momentarily even with no packet loss like around 90 m in Fig. 11(c). It is caused by combination of the RAT switching time (about 35 ms), the difference of processing time and transmission path for each RAT exceeds 100 ms, which is the interval of instantaneous throughput calculation. From the results, it can be seen when switching from mm-com to macro-com, interruption occurs under the terminal-driven scheme, but does not occur under the GW-driven scheme. In addition, as shown in Fig. 10(a), in the terminal-driven, even in the blocking area, since if it is possible to connect to mm-com even for a moment, it switches to mm-com, some round trips between mm-com and macro-com are observed. From the results, it was verified that the GW-driven switch to macro-com, which can switch before entering the mm-wave blocking area, shows superior char-

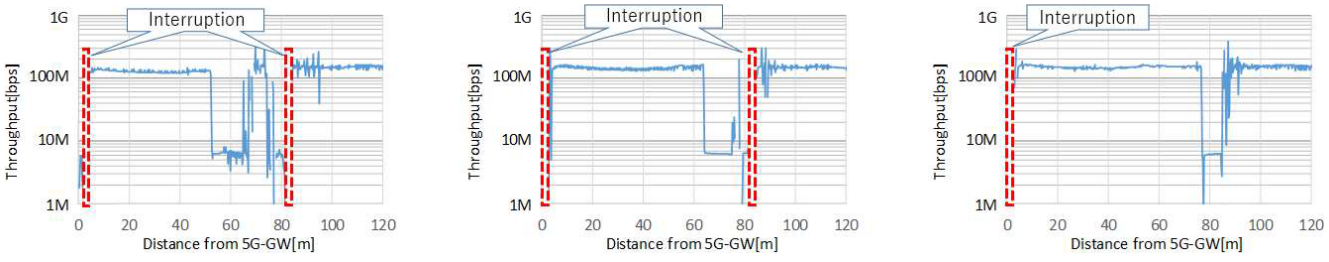

(a)overtaking point=60m (b)overtaking point=74m (c)overtaking point=83m

Fig. 10 Experimental result of the throughput when terminal-driven was used.

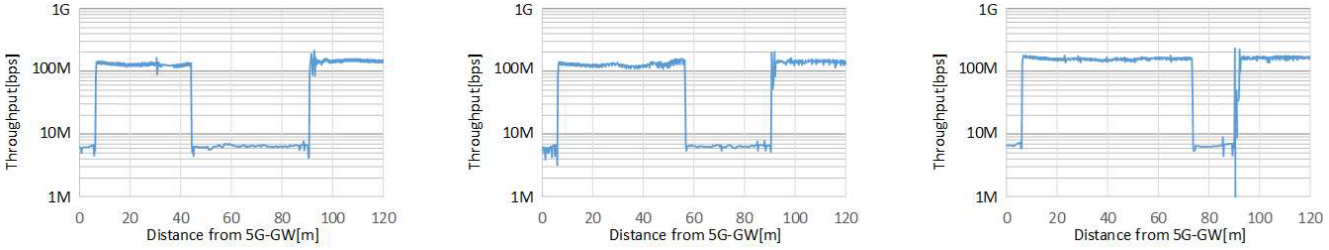

(a)overtaking point=60m (b)overtaking point= 74m (c)overtaking point=83m

Fig. 11 Experimental result of the throughput when GW-driven was used.

acteristics to the terminal-driven device based on the terminal detection by the mm-wave radar.

4.4 Verification of the GW-Driven Scheme

Under the driven of GW, after detection by the mm-wave radar, the route of the terminal is predicted, and based on the communication quality of the mm-wave in the predicted route, it is determined when to switch to macro-com. The quality map shown in Fig. 12 is used at that time. This map is based to use value obtained by simulation, also takes into consideration the blocking area generated by the blocking object and the influencing from the ground reflection, and so on. Therefore, it is necessary to change it sequentially depending on the area situation. However, since in the experiment, the position of the blocking object was fixed, a fixed map was used. Based on this map, 5G-GW predicts when the terminal will enter the low-quality area and informs the suitable switching timing to the terminal. By knowing the optimum switching timing from mm-com to macro-com in advance, the terminal is fully prepared for switching before the switching timing, so there is no momentary interruption during switching.

Figure 13 shows the remaining time overwrote to the throughput characteristics. Remaining time means the difference between the informed suitable switching timing to this terminal and the current time, and the scale of that is on the right side. This figure shows that it is operating of GW-driven correctly because it is switched from mm-com to macro-com at the remaining time=0 at each of the overtaking points 60 m, 74 m, and 83 m, respectively. In GW-driven, after confirming the completion of switching from mm-com to macro-com, prediction of the next switching timing from mm-com to macro-com starts again, regardless of the RAT selection status. Therefore, plots of the remaining time exist around the distance of 60 m in Fig. 13(a), even if the communication status is macro-com.

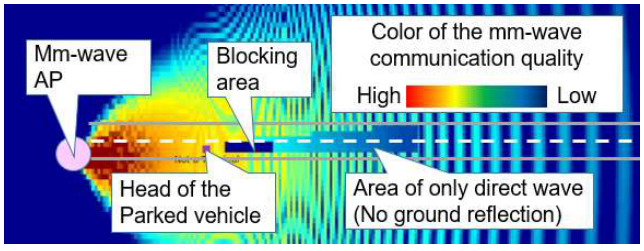

Fig. 12 The quality map use for the GW-driven scheme.

4.5 GW-Driven Scheme with Two Terminals

The above results are that of when there is only one terminal vehicle, but to confirm whether terminal detection and RAT switching work correctly even when multiple terminals exist simultaneously, we added a terminal that downloads (DL) accumulated data is attached. The purpose of this trial is to verify that the point cloud (a set of points represented by direction and distance) acquired by radars can be properly separated and that the accuracy of route prediction for multiple terminals can be maintained respectively. This new additional terminal "Terminal 2" was preceded, and the terminal "Terminal 1" that uploads (UL) the streaming data used in the evaluation in the previous section followed from behind. As shown in Fig. 14, the distance between the two cars was set to 110 m and 35 m, the RAT selection was GW-driven, and the overtaking point was 60 m.

Figure 15 shows the throughput characteristics when the distance between the two vehicles is 110 m. The vertical axis of this figure consists of four stages from the bottom: position of the terminal vehicles in the road width direction (X-axis), position of the terminal vehicles in the road length direction (Y-axis), throughput of the terminal 1, and that of the terminal 2 respectively. The horizontal axis shows the elapsed time from the start of the experiment and is commonly for all stages in this figure. Since download timing of Terminal 2 is planned in a power-efficient location as much as possible, the download was started after overtaking the blocking object. For this reason, in Fig. 15, the download of Terminal 2 was carried out at a point where the position of Terminal 1 was considerably before the overtaking point. On the other hand, when the distance between the two vehicles is 35 m in Fig. 16, the download was carried out at the timing just on the time when the mm-com was switched to the macro-com. In this experiment, since the transmission rate of download is much higher than that of upload, in both cases the throughput of Terminal 1 upload temporarily dropped when Terminal 2 was downloaded, but RAT switching was performed without problems. From this result, it was verified that if the distance between vehicles is about more than 35 m, even if multiple terminal vehi-

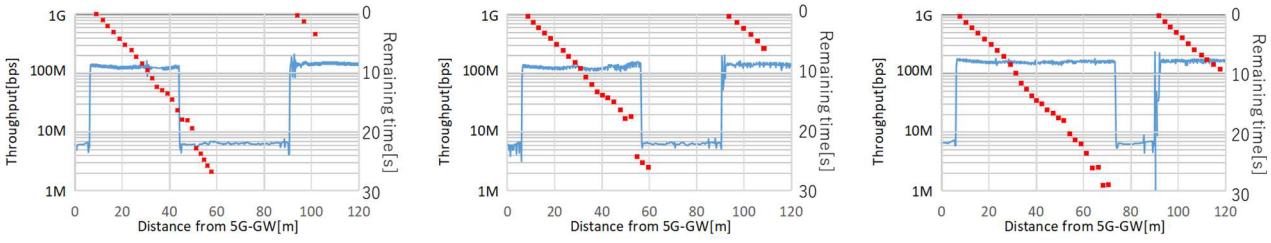

(a)overtaking point=60m (b)overtaking point= 74m (c)overtaking point=83m

Fig. 13 Remaining time with the throughput characteristics.

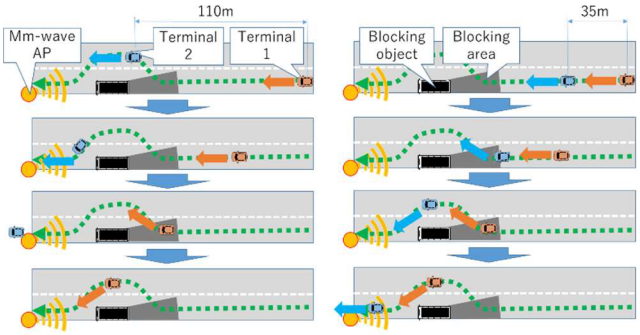

(a) Distance is 110m (b) Distance is 35m

Fig. 14 Route of the two terminals.

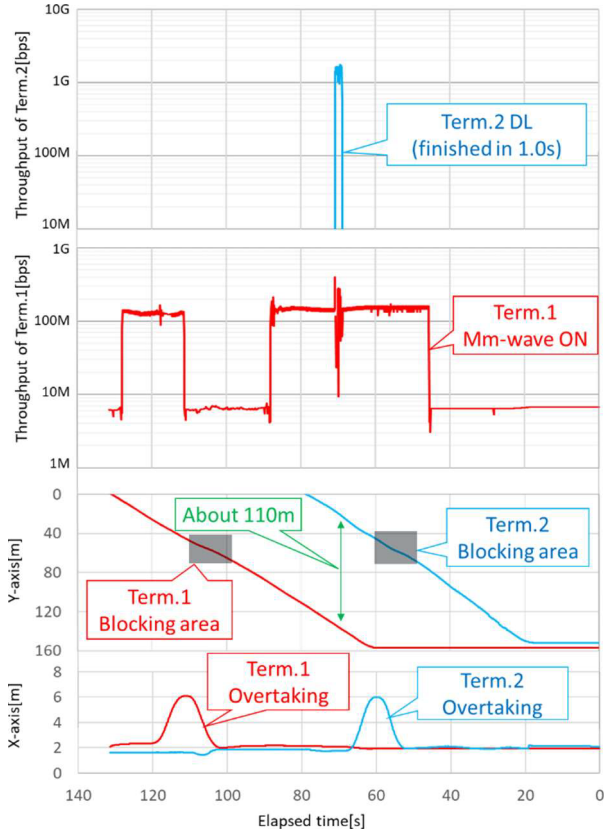

Fig. 15 The throughput characteristics when the distance between the two vehicles is 110 m.

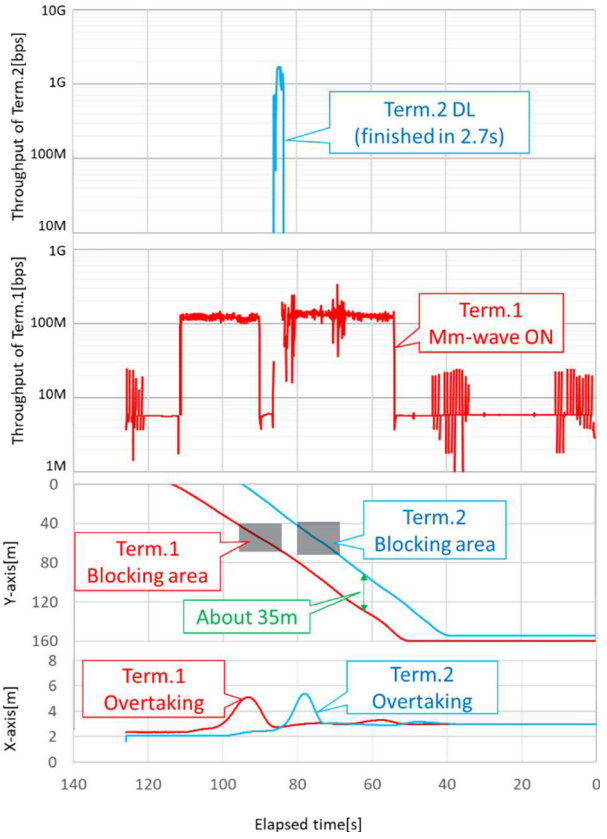

Fig. 16 The throughput characteristics when the distance between the two vehicles is 35 m.

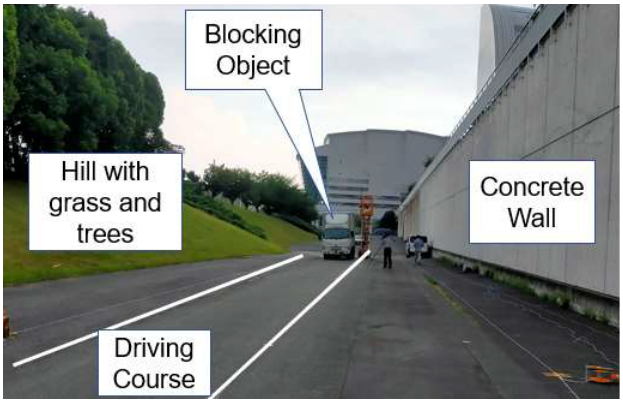

Fig. 17 The experimental course with multi path.

cles are detected simultaneously, terminal identification and RAT switching can be performed without problems.

4.6 GW-Driven Scheme in Multi Path Environment

From the results shown previous section, GW-driven scheme works as expected. However, the environment of the examination was ideal, which means no multi path for mm-com and mm-wave radar. Therefore, we have tried to examine GW-driven scheme in multi path environment as the second trial. Figure 17 shows the experimental scene. There are “concrete wall at right side” and “hill with grass and trees” beside of the course. The height of the wall is about 7 m which is higher than that of mm-wave AP antenna or mm-wave radars.

When multi path exists, not only real objects but also ghosts are observed. For this reason, to select, which point cloud the terminal vehicle performing mm-com belongs to, we decided to perform identification based on the link distance information obtained by mm-com. In addition, parked vehicles and installations on the road are also observed as point clouds, but these are dealt with by removing point clouds that do not move.

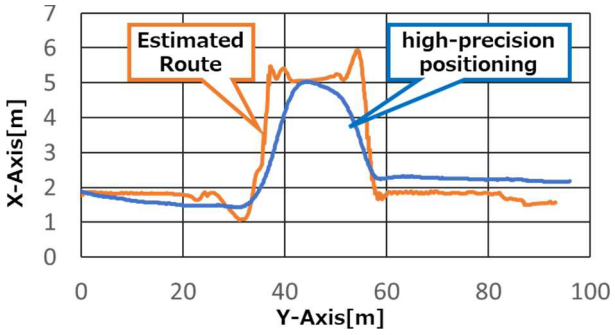

Fig. 18 The comparison between estimated route and the positioning results of high-precision positioning using RTK.

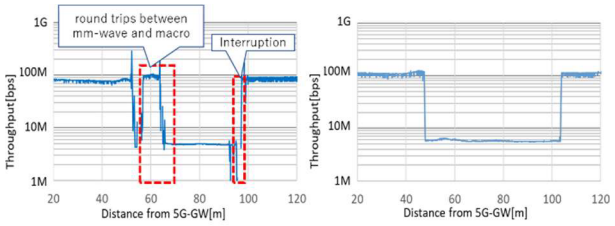

(a)terminal-driven (b)GW-driven

Fig. 19 The throughput characteristics in multi path environment.

Figure 18 is the result of estimating the route while accurately grasping the terminal vehicle by such operations. In Fig. 18, blue line is the positioning results of high-precision positioning using RTK (Real-time Kinematic Positioning) [13] installed in the terminal vehicle and the orange line is the predicted route. The result shows that it was possible to accurately estimate the point where the terminal vehicle overtook a parked vehicles and returned to the previous lane.

Furthermore, the error in route estimation is evaluated by the RMSE (Root Mean Square Error) of the entire driving route. The target value are 3 m in Y-axis that considered from the inter-vehicle distance in normal driving, and 1 m in X-axis that considered from the lane width. The measured values were 2.66 m on the Y-axis and 0.73 m on the X-axis, confirming that they were within the target range even in a multipath environment.

Figure 19 shows the throughput characteristics in multi path environment. The result with terminal-driven (a) has interruption and round trips between mm-com and macro-com, but that with GW-driven (b) has neither interruption nor roundtrip. From the result, GW-driven scheme can work correctly even in multi path environment.

5. Conclusion

Aiming to improve the power efficiency of the 5G system, we are considering a network that uses mm-wave (60 GHz-WLAN) as non-3GPP wireless access systems, which has high power efficiency. As a network configuration, we assumed a configuration in which the macro area overlaps with the mm-wave area, and in areas where mm-waves can be used, we decided to choose the optimum RAT selection scheme which can use mm-waves as much as possible. However, because of the blocking problem, momentary interruptions when switching between RATs or unstable communication due to round trips between RATs may occur. Therefore, we devised a GW-driven scheme that predicts the route of the terminal using radar and switches from mm-com to macro-com before it leaves the mm-wave area, implemented it on a prototype device, and confirmed its characteristics. First, we evaluated the characteristics of the GW-driven in an environment without multi path, then we evaluated the characteristics of the GW-driven in an urban model where there are walls and hills on the left and right sides of the road. From the results, we confirm that optimal RAT selection with GW-driven can be achieved even in a multi path environment. In the next step, we plan to confirm that the optimum RAT selection with GW-driven can also work well for handover between mm-wave areas without interruption in an environment where mm-wave areas are continuous.

Acknowledgments

This work was supported by “Research and development project for expansion of radio spectrum resources” of MIC, Japan (JPJ000254).

References

[1] IEEE 802.11 Working Group. IEEE Standard for Information Technology–Telecommunications and Information Exchange between Systems–Local and Metropolitan Area Networks–Specific Requirements–Part 11: Wireless LAN Medium Access Control (MAC) and Physical Layer (PHY) Specifications Amendment 3: Enhancements for Very High Throughput in the 60 GHz Band. IEEE Std, 802.11ad, 2012.

[2] 3rd Generation Partnership Project; Technical Specification Group Services and System Aspects, “System architecture for the 5G system (5GS); Stage 2,” 3GPP TS23.501, V17.5.0, June 2022.

[3] T. Suzuyama, H. Ohue, S. Imaizumi, N. Shimizu, T. Asanuma, and H. Asano, “Simulation-based evaluation of energy efficiency for millimeter-wave network,” IEICE Commun. Express, vol.11, no.12, pp.823–828, 2022.

[4] K. Sakaguchi, R. Fukatsu, T. Yu, E. Fukuda, K. Mahler, R. Heath, T. Fujii, K. Takahashi, A. Khoryaev, S. Nagata, and T. Shimizu, “Towards mmWave V2X in 5G and beyond to support automated driving,” IEICE Trans. Commun., vol.E104-B, no.6, pp.587–603, June 2021.

[5] V. Thenmozhi and M. Bhaskar, “A 60-GHZ low-noise amplifier with +7.258-dBm third-order input intercept point using current reuse feedforward distortion cancellation for 5G emerging communication,” International Journal of Circuit Theory and Application, vol.50, no.6, pp.1855–1875, 2022.

[6] Z. Kasfia and M.M. Munjure, “A millimeter wave fronthauling solution for open RAN paradigm in 5G and beyond networks,” IEEE Conference Proceedings, vol.2021, no.ICTP, pp.1–5, 2021.

[7] R. Mehrotra, R.I. Ansari, A. Pitilakis, S. Nie, C. Liaskos, N.V. Kantartzis, and A. Pitsillides, “3D channel modeling and characterization for hypersurface empowered indoor environment at 60 GHz millimeter-wave band,” IEEE Conference Proceedings, vol.2019, no.SPECTS, pp.1–6, 2019.

[8] H. Asano, H. Noguchi, N. Shimizu, T. Asanuma, M. Yasugi, T. Ueta, K. Ohno, and R. Honda, “High power efficiency millimeter-wave network with communication quality prediction technology,”

17th IEEE VTS Asia Pacific Wireless Communications Symposium (APWCS), S2-6, 2021.
[9] T. Ueta, T. Okada, K. Ono, M. Uesugi, Y. Shinagawa, and K. Kosaka, "Estimation position in the shield area using route information in wireless communication control," IEICE General Conference, B-5-39, March 2022.
[10] S. Ono, M. Umehira, S. Takeda, T. Miyajima, and K. Kagoshima, "Temporal and frequency characteristics of shadowing by Human Body in 60GHz WLAN," IEICE Technical Report, SIP2013 85-135, Jan. 2014.
[11] K. Yoshikawa, S. Mihara, T. Murakami, and H. Shinbo, "Machine learning using top view for prediction of blocking effect of millimeter-wave to moving terminal," IEICE Society Conference, B-5-52, Aug. 2021.
[12] Y. Koda, K. Yamamoto, T. Nishio, and M. Morikura, "Experimental evaluation of reinforcement learning-based pedestrian-aware predictive handover for mmWave networks," IEICE Technical Report, RCC2018 25-57 July 2018.
[13] J. Wanninger, "Introduction to nework RTK," IAG Working Group 4.5.1: Network RTK (2003–2007), June 2008. http://www.wasoft.de/e/iagwg451/intro/introduction.html

Mitsuru Uesugi received his B.E. degree from the Waseda University, Tokyo, Japan, in 1986, and his Ph.D. degree in engineering from the Tohoku University, Miyagi, Japan, in 2004. Since 1986, he has been engaged in the research and development of wireless communication technologies for 2G, 3G, 4G, 5G, LPWA and RFID at Panasonic Group, Kanagawa, Japan.

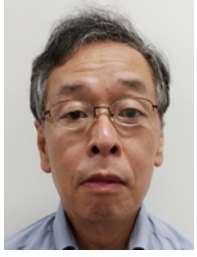

Yoshiaki Shinagawa received his M.S. degree in engineering from Tokai University, Tokyo, Japan, in 1988. Since 1988, he has been engaged in the research and development of wireless communication technologies for 2G, 3G, 5G and LPWA at Panasonic Group, Kanagawa, Japan.

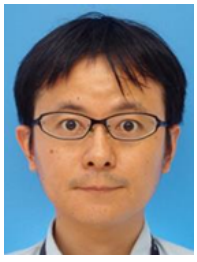

Kazuhiro Kosaka received the M.S. degree in electrical and electronic engineering from Tokyo Institute of Technology, Tokyo, Japan, in 2003. In 2003, he joined Panasonic Mobile Communications Co., Ltd., where he was engaged in the development and electronic circuit design of mobile communication technologies for GSM, 3G and LTE. From 2012 to 2015, he was engaged in research on the advanced technology of OFDM wireless communication systems at the Advanced Telecommunications Research Institute International (ATR). Since 2015, he has been engaged in the research and development of wireless communication technologies for Microwave link, LPWA and 5G at Panasonic Group, Kanagawa, Japan.

Toru Okada received B.E. in engineering from University of Erectro-Communications, Tokyo Japan in 1990. In 1990, he joined Matsushita communication Ind. Co., Ltd., where he engaged in research for modulation scheme and development of test system for mobile wireless system such as Personal Handy phone, 3G, 4G, and 5G cellular phone. Since 2008, he has been engaged in the research and development of wireless sensor systems such as UWB wireless tag system, microwave RADAR system and milli-meter RADAR system at Panasonic Group, Kanagawa, Japan.

Takeo Ueta received the M.S. degree in electronic material science from Shizuoka University, Shizuoka, Japan, in 2016. In 2016, he joined Panasonic Co., Ltd. From 2016 to 2018 he was engaged in the research and development of millimeter wave communication technologies for backhaul line at Osaka, Japan. Since 2019, he has been engaged in the research and development of millimeter wave radar technologies for detect objects and estimate vital information at Kanagawa, Japan. And, since 2022, he also has been engaged in the research and development of CG technologies for image processing.

Kosuke Ono received the B.E. degree from Keio University, Tokyo, Japan, in 2016. In 2016, he joined Panasonic Co., Ltd. From 2016 to 2018 he was engaged in the research and development of the storage system at Osaka, Japan. Since 2019, he has been engaged in the research and development of millimeter wave radar technologies for detect objects and estimate vital information at Kanagawa, Japan. And, since 2022, he also has been engaged in the research and development of CG technologies for image processing.